Characterization of Unique DNA-Binding and Transcriptional-Activation Functions in the Carboxyl-Terminal Extension of the Zinc Finger Region in the Human Vitamin D Receptor†

Jui-Cheng Hsieh, G. Kerr Whitfield, Anish K. Oza, Hope T. L. Dang, Jack N. Price, Michael A. Galligan, Peter W. Jurutka, Paul D. Thompson, Carol A. Haussler, and Mark R. Haussler*

Department of Biochemistry, College of Medicine, The University of Arizona, Tucson, Arizona 85724

Received July 19, 1999; Revised Manuscript Received September 27, 1999

ABSTRACT: The vitamin D receptor (VDR) binds 1,25-dihydroxyvitamin D_3 and mediates its actions on gene transcription by heterodimerizing with retinoid X receptors (RXRs) on direct repeat (DR+3) vitamin D responsive elements (VDREs) located in target genes. The VDRE binding function of VDR has been primarily ascribed to the zinc finger region (residues 24−87). To define the minimal VDRE binding domain for human VDR (hVDR), a series of C-terminally truncated hVDR mutants (Δ134, Δ113, Δ102, Δ90, Δ84, Δ80, and Δ60) was generated and expressed in bacteria. Only the Δ134 and Δ113 mutants bound the VDRE (predominantly as monomers), suggesting that, in addition to the conserved zinc finger region of hVDR, as many as 25 amino acids in a C-terminal extension (CTE) participate in DNA binding. Site-directed mutagenesis of conserved charged residues in full-length hVDR was then performed to dissect the functional significance of the CTE (residues 88−112) in the context of the complete hVDR−RXR−VDRE interaction. Functional assays revealed that E98K/E99K, R102A/K103A/R104A, and K109A/R110A/K111A mutant hVDRs possessed dramatically reduced DNA binding and transcriptional activities, whereas distinct point mutants, such as K103A, bound to DNA normally but lacked transcriptional activity. Therefore, the boundary for the minimal DNA-binding domain in hVDR extends C-terminal of the zinc fingers to Lys-111, with clusters of highly conserved charged amino acids playing a crucial role in binding to the DR+3 element. Further, individual residues in this region (e.g., Lys-103) may lie on the opposing face of a DNA-binding α-helix, where they could contact transcriptional coactivators or basal transcription factors.

The VDR[1] is a nuclear protein that belongs to the superfamily of transcription factors, including the steroid, retinoid, and thyroid hormone receptors (*1*, *2*). VDR mediates the hormonal response to 1,25-dihydroxyvitamin D_3 (1,25-$(OH)_2D_3$), the active metabolite of vitamin D, by binding as a heterodimer with the RXR to specific VDREs located within the 5′-promoter region of target genes, such as rat and human osteocalcin (*3*−*5*), mouse osteopontin (*6*), avian integrin β_3 (*7*), and rat vitamin D 24-hydroxylase (*8*, *9*).

In common with other members of the nuclear receptor superfamily, the VDR protein possesses a modular configuration consisting of a number of distinct domains that reflect, on a structural level, the molecular actions of VDR in response to its ligand. Thus, the fundamental arrangement of VDR can be described as consisting of an N-terminal DNA-binding domain, a C-terminal hormone binding domain, and heterodimerization and transactivation domains comprised primarily of subregions within the hormone binding segment (*2*, *10*). Of all these regions, the DNA-binding domain (DBD), including two zinc finger motifs of the C4 type, displays the highest degree of conservation throughout the nuclear receptor superfamily (*10*), with the homology extending some distance past the last conserved cysteine (see Figure 8). The degree of conservation is high enough to suggest that the same general structural features are present throughout the superfamily. An initial approximation of these structural features is provided by the availability of the cocrystal structure for the DBDs of thyroid hormone receptor and RXR bound as a heterodimer to the thyroid hormone responsive element (TRE) (*11*). This X-ray crystallographic study demonstrates the presence of an α-helix on the C-terminal side of each zinc finger, with helix A and helix B forming the DNA recognition and phosphate backbone binding helices, respectively. Specific evidence for structural congruity between the zinc finger regions of VDR and thyroid hormone receptor (TR) is further provided by a

† Supported by NIH grants to J.-C. H. and M. R. H.

* Address correspondence to Mark R. Haussler, Ph.D., Department of Biochemistry, College of Medicine, The University of Arizona, Tucson, AZ 85724. Telephone: 520-626-6033. Fax: 520-626-9015. E-mail: haussler@u.arizona.edu.

[1] Abbreviations: VDR, vitamin D receptor; RXRs, retinoid X receptors; DR+3, direct repeat with spacer of 3 bp; VDREs, vitamin D responsive elements; hVDR, human vitamin D receptor; CTE, C-terminal extension; $1,25(OH)_2D_3$, 1,25-dihydroxyvitamin D_3; DBD, DNA-binding domain; TRE, thyroid hormone responsive element; TR, thyroid hormone receptor; HVDRR, hereditary hypocalcemic vitamin D-resistant rickets; GR, glucocorticoid receptor; ER, estrogen receptor; RAR, retinoic acid receptor; RXRE, RXR responsive element; hERR2, human estrogen-receptor related receptor 2; PPARs, peroxisome proliferator-activated receptors; IPTG, isopropyl-β-D-thiogalactoside; PBS, phosphate buffered saline; PXR, pregnane X receptor; dUSP, *Drosophila ultraspiracle*.

10.1021/bi9916574 CCC: $18.00
Published on Web 11/12/1999

number of naturally occurring missense mutations within this domain of VDR (His-35, Lys-45, Arg-50, Arg-73, and Arg-80) that are known to correspond to DNA contacts in the TR−RXR−TRE crystal structure (*2*, *12*). Each of these natural mutations in hVDR results in the clinical condition of hereditary hypocalcemic vitamin D-resistant rickets (HVDRR), characterized by a tissue insensitivity to 1,25-$(OH)_2D_3$, strongly arguing for a crucial functional role for these residues.

The DNA-binding domain of VDR possesses a unique feature among the nuclear receptors in that there exists between the two zinc fingers a cluster of five basic amino acids (positions 49−55) that has been shown to be critical for nuclear localization (*13*). This segment of the VDR DBD also contains a phosphorylation site (Ser-51) for protein kinase C (*14*). Phosphorylation of this residue results in an inhibition of VDRE binding, thus indicating that both the DNA binding and nuclear localization properties of VDR, in vivo, may be modulated by posttranslational modification of the zinc finger region in a way somewhat distinct from other superfamily members (*15*).

There also appears to be considerable variation throughout the nuclear receptor superfamily as to the functional role(s) of non-zinc finger residues in the C-terminal extension of the zinc finger core. While the minimal DBDs of the glucocorticoid receptor (GR) (*16*), estrogen receptor (ER) (*17*), retinoic acid receptor (RAR) (*18*), and RXR (*19*) have been reported to extend from the first cysteine to 13−17 residues C-terminal of helix B, the minimal TR DBD appears to be significantly longer and encompasses at least 31 residues extending from helix B (*11*). Thus, while many receptors appear to require a CTE for DNA binding, the exact length of the required CTE is variable between receptors.

Two functional subdomains have been proposed within the CTE region of nuclear receptors (*20*). These were termed the T-box, originally described for mouse RXRβ, and the A-box, delineated in the orphan receptor NGFI-B. The structure and precise molecular actions of these subdomains appear to vary according to the DNA binding and dimerization characteristics of each receptor. For example, the T-box of RXRα is α-helical and defines a structural feature required for the cooperative dimerization of RXRα on a responsive element possessing a direct repeat structure (*19*). In contrast, the cocrystal structure of the TR−RXR−DNA complex reveals that the CTE of TR, while containing a small α-helix at the N-terminus of the T-box that generates a dimer interface, also forms a connecting loop to a second α-helix encompassing, but extending beyond, the A-box. This second α-helix in TR forms extensive nonspecific DNA backbone and minor groove interactions (*11*). Further, this structure is postulated to be the key element that precludes formation of TR−RXR on direct repeats spaced by less than four base pairs (*11*).

With respect to the role of the A-box in receptors that bind DNA only as monomers, namely, NGFI-B, Rev-ErbA, and ROR, this region effects highly sequence-specific DNA binding through contacts with 5′ extensions of the respective responsive elements (*21*−*23*). Thus, even receptors binding to monomeric elements require a CTE, particularly for interaction with bases 5′ of the consensus hexanucleotide half-element.

In the case of VDR, there have been several studies utilizing C-terminal truncation mutants that have alluded to the requirement of the CTE for DNA binding. We have previously reported that an hVDR truncation mutant (Δ134), which contains 130 amino acids from residue 4 to 133, displayed DNA-binding activity that was independent of the RXR heterodimeric partner (*24*). Similar results were obtained by others using an hVDR fragment termed VDRF, containing 100 amino acids beginning at residue 15 and ending at residue 114 (*25*), and also during the characterization of two C-terminal truncation mutants of hVDR, Δ114−427 and Δ190−427 (*26*). In combination, these functional data implied that the DBD of hVDR may extend beyond the zinc finger core, which consists of residues 24−87. In the present study, we sought to define more precisely the minimal DBD of hVDR, and to evaluate the potential roles of the T- and A-boxes present within the CTE. Evidence is provided that in the context of the full-length hVDR, the T- and A-boxes, as well as sequences extending further C-terminal of the A-box, are crucial in conferring both the DNA-binding and transcriptional activation properties of this receptor.

MATERIALS AND METHODS

In Vitro Site-Directed Mutagenesis. Mutagenic oligonucleotides were used to generate hVDR C-terminal truncation mutants (i.e., Δ60, Δ80, Δ84, Δ90, Δ102, Δ113, and Δ134), the K82E helix B mutant and the E98K/E99K double mutant in the T-box, the A-box mutants (i.e., R102G, K103G, R104G, R102A/K103A, R102A/K103A/R104A, E105G, M106G, I107G, and ΔA-box), the flanking mutants C-terminal of the A-box (i.e., K109G/R110G/K111G, K109A/R110A/K111A, and E112G), and the first zinc finger mutants (i.e., loop IA and loop IB) by site-directed mutagenesis as described previously (*14*). One T-box mutant discussed in the present study, namely, K91N/E92Q, was created and evaluated previously (*27*).

Overexpression of Truncated Mutants in Escherichia coli and Cell Extract Preparation. The pT7-7hVDR plasmid (*24*) contains a wild-type hVDR cDNA, a T7 RNA polymerase promoter denoted ø10, which is positioned 5′ of a polylinker sequence, and the translation start site for the T7 gene ø10 protein. This pT7-7hVDR plasmid was utilized to create the truncation mutants Δ60, Δ80, Δ84, Δ90, Δ102, Δ113, and Δ134. The resulting constructs were transformed into *E. coli* BL21(DE3)plysS, which contains a genomic copy of the viral T7 RNA polymerase under the control of an IPTG-inducible UV5 promoter. The bacterial cells were grown in 3 mL of TB medium (12 g/L bacto tryptone, 24 g/L bacto yeast extract, 4 mL/L glycerol, 2.31 g/L KH_2PO_4, 1.54 g/L K_2HPO_4) with ampicillin (100 μg/mL) and chloramphenicol (25 μg/mL) at 37 °C. At an absorbance (590 nm) of 0.20, IPTG was added to a final concentration of 0.3 mM. Cells were harvested after further incubation at 37 °C for 2 h. The cell pellet was suspended in 500 μL of buffer containing 10% glycerol, 50 mM Tris/HCl pH 7.5, 1 mM EDTA, 1 mM DTT, 2.5 μg/mL E-64, 200 μg/mL pefabloc SC (Roche Molecular Biochemicals, Indianapolis, IN), 1 μg/mL pepstatin, 2 μg/mL aprotinin, and 1 μg/mL leupeptin. After a 10 min incubation, the suspension was sonicated for 45 s and centrifuged at 16000*g* at 4 °C for 5 min. The supernatant

was stored at −80 °C for subsequent determination of the protein concentration and for use in the gel mobility shift assay.

Gel Mobility Shift Assay. The synthetic oligonucleotide CT5, 5′-AGCTGCACT*GGGTGA*ATG*AGGACA*TTACA-3′, containing the DR+3 VDRE sequence (in italics) from the rat osteocalcin gene (*5*), was utilized as the probe. Double-stranded CT5 oligonucleotide was labeled with [α-^{32}P]dCTP (3000 Ci/mmol) at the 5′-overhanging ends with the Klenow fragment of DNA polymerase I to a specific activity of $>10^8$ cpm/μg DNA. Whole cell extracts of the truncated mutants, Δ60, Δ80, Δ84, Δ90, Δ102, Δ113, and Δ134, were prepared from IPTG-induced bacteria (described above), and directly incubated with CT5 probe without RXRα. All hVDR point mutants used in the gel mobility shift assay were obtained from whole cell extracts of COS-7 cells transfected with wild-type or mutant pSG5hVDR plasmids (described below). *E. coli*-expressed human RXRα was preincubated with the hVDR from COS-7 cell extracts in DNA-binding buffer (10 mM Tris-HCl, pH 7.6, 150 mM KCl, 2 μg of bovine serum albumin, and 1 μg of poly (dI-dC)) for 15 min at 22 °C and then incubated with 0.5 ng of ^{32}P-labeled probe for an additional 15 min. The reaction mixtures were loaded onto 4% nondenaturing polyacrylamide gels containing 22.5 mM Tris-borate, pH 7.2, 0.5 mM EDTA. Gels were run at 10 mA for 70 min, dried, and exposed for autoradiography.

Cotransfection of COS-7 Cells and Transcription Assays. Transcriptional activity was measured in COS-7 cells. These cells were cotransfected in duplicate by the calcium phosphate DNA coprecipitation method (*14*) with the various pSG5hVDR expression plasmids, pTZ18U as carrier DNA, and the rat osteocalcin VDRE-containing reporter plasmid $(CT4)_4$TKGH (*5*). Cells were treated for 24 h following transfection with either 10 nM $1,25(OH)_2D_3$, or ethanol (vehicle) as a control. The media were assayed by radioimmunoassay for the expression of hGH using a kit from Nichols Institute Diagnostics (San Juan Capistrano, CA) and the data expressed as mean ± standard deviation. The cells were then scraped, washed three times with PBS (136 mM NaCl, 26 mM KCl, 8 mM Na_2HPO_4, and 1.5 mM KH_2PO_4, pH 7.2), and suspended in KETD-0.3 buffer (10 mM Tris-HCl, pH 7.2, 1 mM EDTA, 300 mM KCl, 10% glycerol, 1 mM DTT, 0.1 mM phenylmethylsulfonylfluoride, 15 μg/mL aprotinin, 1 μg/mL leupeptin, and 1 μg/mL pepstatin-A). After sonication, samples were centrifuged at 16000*g* for 15 min at 4 °C. Protein concentrations were determined according to the method of Bradford (*28*). Immunoblotting of cell extracts was performed as previously described (*13*) with minor modifications. First, 24 μL of neutravidin and 6 μL of biotinylated alkaline phosphatase (Bio-Rad, Hercules, CA) were added to 5 mL of 1% blotto, premixed for 45 min at room temperature, and then diluted to 30 mL with 1% blotto prior to incubation with the membrane for 2 h. Second, although anti-VDR monoclonal antibody 9A7γ was used in most experiments, a polyclonal anti-VDR antibody directed against an epitope near the C-terminus (Affinity BioReagents, Golden, CO) was used at a dilution of 1:500 to verify the expression of several mutant VDRs wherein the 9A7γ epitope was compromised (see Table 1).

Protein Expression via In Vitro Transcription/Translation. hVDR protein synthesis from the T7 promoter in pSG5hVDR was performed using a TNT-coupled reticulocyte lysate system kit (Promega, Madison, WI), according to the protocol of the manufacturer. Briefly, master mix was first prepared with the following components of the kit: 12 μL of TNT buffer; 6 μL of amino acid mix; 6 μL of RNAsin; 3 μL of Pefabloc SC; 3 μL of leupeptin/aprotinin; 13.8 μL of double distilled water; 24 μL of ^{35}S-methionine (1200 Ci/mmol at 10 mCi/ml); 10.2 μL of T7-polymerase; and 174 μL of rabbit reticulocyte lysate. One microgram of wild-type or mutant circular pSG5hVDR was added directly to the TNT master mix and incubated in a 50 μL reaction for 1.5 h at 30 °C. The final translation products were analyzed on a 10% SDS/polyacrylamide gel. After electrophoresis, gels were fixed, dried, and exposed to Kodak XAR film at −70 °C.

Table 1: Summary of the Phenotypes of Helix B and CTE Mutant hVDRs; Refinement of the 9A7γ Epitope

mutant	VDRE binding[a]	transcription[a]	recognition by 9A7γ
wild-type	++++	++++	Yes
K82E	++	++	Yes
K91N/E92Q	+	+	Yes
E98K/E99K	+	−	No[c]
R102G	++++	+	Yes
R102A[b]	++++	++	Yes
K103G	++++	+	Yes
K103A[b]	+++	−	Yes
R102A/K103A[b]	++++	−	Yes
R104G	++++	+	No[c]
R104A[b]	++++	+	No[c]
R102A/K103A/R104A	+	+	No[c]
E105G	degraded	degraded	Yes[d]
M106G	++++	++	Yes
I107G	++++	++	Yes
K109A[b]	+++	++	Yes
R110A[b]	+++	+	Yes
K111A[b]	+++	+	Yes
K109G/R110G/K111G	+	−	Yes
K109A/R110A/K111A	+	+	Yes
E112G	++++	++++	Yes

[a] Relative activity compared with wild-type is as follows: ++++, 75−100%; +++, 50−75%; ++, 25−50%; +, 5−25%; −, 0−5%. [b] Not shown in Figure 1E. [c] Expression was verified via immunoblots utilizing a polyclonal antiserum directed against the C-terminus of VDR. [d] 15 kDa fragment visualized.

RESULTS

Initial evaluation of the DNA-binding domain of hVDR was carried out by generating a series of C-terminal truncations (Figure 1A), beginning with Δ134 and Δ113, which have previously been shown to possess intrinsic DNA-binding activity (*24*−*26*), continuing with a novel series, including Δ102, Δ90, Δ84 and Δ80, progressively removing the C-terminal extension and portions of helix B of the second zinc finger (Figure 1E), and finally terminating with Δ60 hVDR, which lacks the entire second zinc finger. Figure 1B illustrates that, by gel shift analysis, Δ134 and Δ113 hVDRs are capable of binding as monomers to the rat osteocalcin VDRE, but Δ102 displays little or no apparent association with this VDRE. Further truncations (Δ90, Δ84, Δ80, and Δ60) also exhibited no detectable binding to the VDRE by gel shift analysis (data not shown). Verification that Δ102 is incapable of VDRE binding, while Δ113 associates with this element as a monomer was achieved by repeating the experiment of Figure 1B with these two truncated hVDRs, including extracts from cells not treated

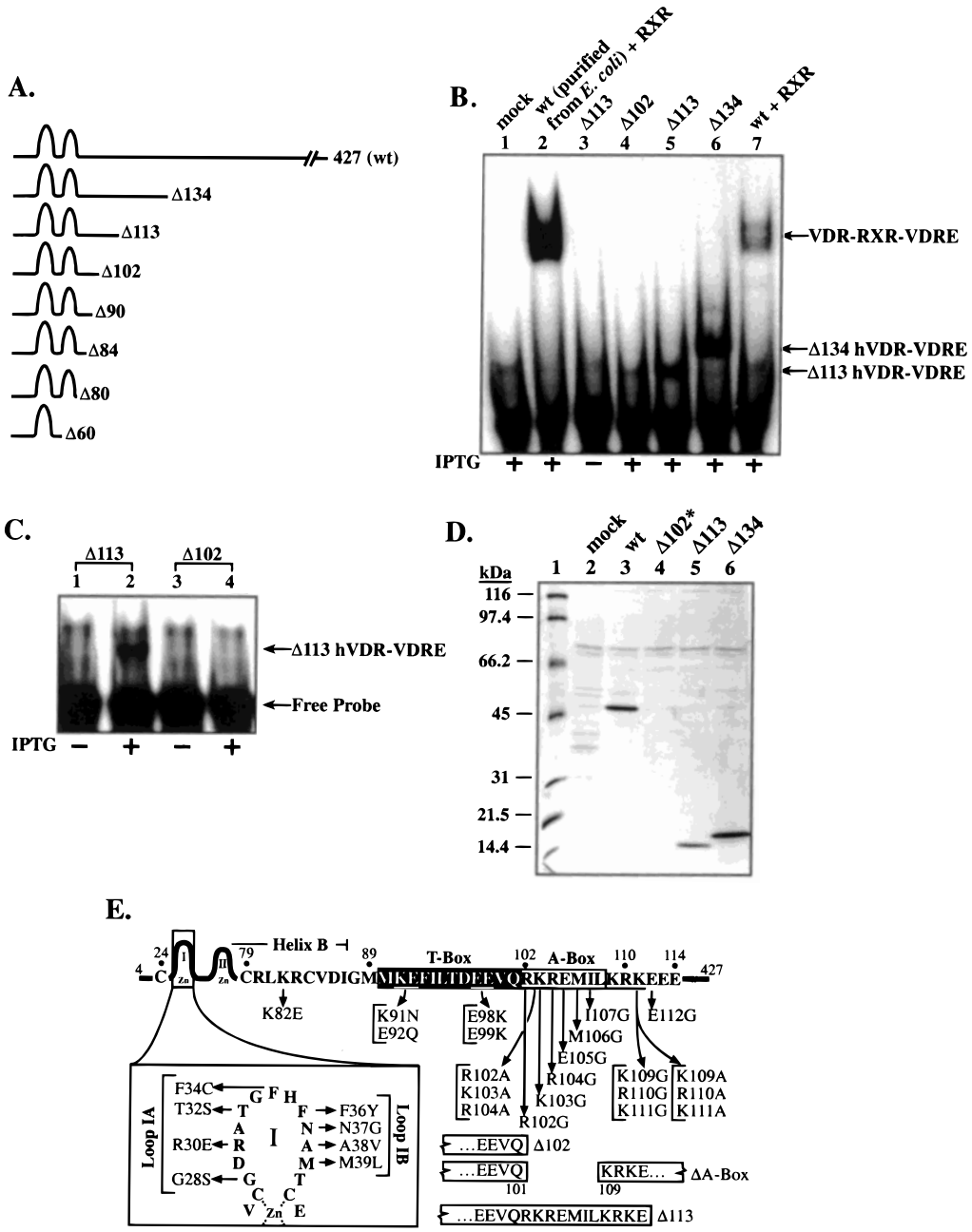

FIGURE 1: Estimation of the minimal DNA-binding domain of hVDR by truncation analysis. (A) Schematic depiction of the C-terminal hVDR truncations tested. hVDR amino acid residue 1 corresponds to methionine 1 of Baker et al. (*41*). (B) DNA-binding activity of hVDR C-terminal truncations by gel mobility shift analysis. Whole cell extracts (5 μg protein) containing the indicated truncated hVDRs, produced in the pT7−7 *E. coli* overexpression system in the presence of IPTG, were incubated with labeled CT5 rat osteocalcin VDRE probe. Lane 1: Mock transformation of *E. coli* as a negative control. Lane 2: Purified *E. coli*-expressed wild-type hVDR (60 ng) incubated with purified *E. coli*-expressed RXRα (50 ng) as a positive control. Lane 3: Δ113 expressed without IPTG induction as a negative control for lane 5. Lanes 4−6: Indicated hVDR truncation mutant expressed in the presence of IPTG. Lane 7: Whole cell extract of *E. coli* expressing wild-type (wt) hVDR with RXRα added prior to DNA binding. (C) Additional evaluation of Δ113 and Δ102 hVDRs for DNA binding. The experiment was performed similarly to that described in B, without IPTG induction in lanes 1 and 3, and 2 h with IPTG in the *E. coli* expression system in lanes 2 and 4. Electrophoresis was in a 5% nondenaturing polyacrylamide gel in this experiment only. (D) Expression of wild-type and truncated hVDRs as determined by immunoblot analysis. Transfected COS-7 cell extracts (40 μg total protein) were loaded onto a 5−15% gradient SDS-polyacrylamide gel, followed by Western blot analysis utilizing 9A7γ primary antibody (*13*). Molecular weight standards are shown in lane 1. Lane 4: Δ102* truncated mutant hVDR is marked by asterisk (*) to indicate that it was not detectable in the Western blot due to the partial loss of the 9A7γ antibody epitope (see Figure 3C). (E) Mutations in the minimal DNA-binding region that were evaluated in the context of full-length (4−427) hVDR. Shown is a schematic view of the N-terminal zinc finger region and its C-terminal extension. The darkened rectangle represents the T-box, involved in heterodimerization with RXR (Lys-91 and Glu-92) (*27*) and possibly in DNA binding. The open rectangle outlines the A-box, a helical region participating in DNA binding by NGFI-B orphan receptor monomers (*20*). Single point mutant hVDRs are generally designated by a straight arrow from the residue altered; double and triple point mutant amino acids are underlined in the primary sequence and designated with curved arrows to a bracketed notation. In the lower right, the two key C-terminal hVDR truncations (Δ102 and Δ113) and a deletion mutant (ΔA-box) are depicted. Shown in the lower left box are two quadruple mutant hVDRs that were constructed to examine the contribution to VDRE binding of the loop of the first zinc finger. For loop IA and loop IB VDR mutants, four amino acids in either half of the first loop were altered to the corresponding four residues in the mouse glucocorticoid receptor.

with the IPTG inducing agent as negative controls (Figure 1C). The combined results of Figure 1, B and C, indicate that amino acids between position 102 and 112 of VDR are crucial for the VDRE-binding function of the receptor. However, because the epitope for the monoclonal antibody (9A7γ) used in immunoblot detection of expressed hVDRs encompasses residues 93−104 (see Figure 3C, below), it was not possible to verify the expression and stability of truncated receptors smaller than Δ113 by this method (Figure 1D). Therefore, all truncations, including Δ102 hVDR, were expressed in the IPTG-induced *E. coli* system and assessed by denaturing polyacrylamide gel electrophoresis and Coomassie Blue staining (data not shown), confirming expression of all mutant VDRs.

To extend the hVDR truncation results and examine the involvement of the zinc finger region and its CTE in DNA binding within the context of the full-length receptor heterodimerized with RXR, we next constructed a number of mutations in the CTE of hVDR 4−427. Figure 1E depicts an ensemble of single, double, triple, and quadruple point mutants as well as a small internal deletant (ΔA-box), that were engineered in full-length hVDR. These mutations were targeted to the first zinc finger (loop IA and loop IB), helix B of the second zinc finger (K82E), and especially concentrated in conserved charged CTE residues between Gly-88 and Glu-112. The region dissected included the T-box (residues 90−101), previously shown to be involved in VDR heterodimerization with RXR (*11*, *27*), as well as the A-box (residues 102−108), an α-helical domain participating in DNA binding by NGFI-B orphan receptor monomers (*20*). The mutated hVDRs in Figure 1E were transfected into COS-7 cells, and their abilities to bind to, and to activate transcription from, the rat osteocalcin VDRE were then assessed.

As shown in Figure 2A, DNA binding/RXR heterodimerization is compromised by the deletion of the A-box in hVDR, an effect duplicated by mutation of two glutamic acids (residues 98 and 99) in the T-box. Not surprisingly, the A- and T-box mutations elicit a reduction of VDR transcriptional activity corresponding to their impairment of DNA-binding (Figure 2B). A somewhat different pattern is seen with the loop I mutants. DNA binding by hVDR is virtually unaffected by loop I alterations that maintain the general zinc finger motif. Interestingly, these same loop I hVDR alterations significantly decreased the transactivation capacity of the receptor, possibly revealing the importance of unique residues in the first zinc finger in contacting transcription coactivators or basal factors (Figure 2B). All mutant hVDRs investigated in the experiments portrayed in Figure 2, A and B, were reasonably well-expressed (Figure 2C), although we were unable to detect E98K/E99K hVDR, because of an apparent disruption of the antibody epitope (see Figure 3C, below). To ensure that the T-box mutant hVDR, E98K/E99K, was properly synthesized, in vitro transcription/translation of this construct was performed. As is evident from Figure 3B, ^{35}S-methionine-labeled E98K/E99K hVDR is synthesized with an efficiency that approaches that of wild-type hVDR in this in vitro system.

Before probing single point mutations within the hVDR A-box for functional activities, we first evaluated the expression and stability of these altered hVDRs. Figure 3A shows via immunoblot analysis that point mutation of Arg-102, Lys-103, Met-106, or Ile-107 to glycine alters neither the expression nor stability of hVDR. In contrast, R104G hVDR cannot be visualized by Western blot, and the E105G mutation renders the receptor susceptible to proteolysis to a 15 kDa immunoreactive fragment. A complementary in vitro

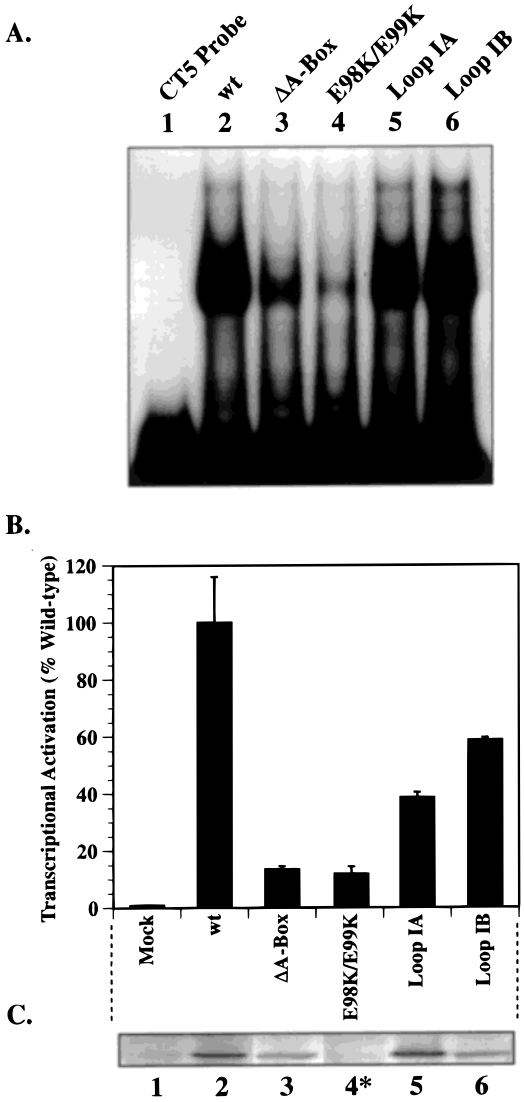

FIGURE 2: VDRE-binding and transcriptional activation capacities of wild-type and mutant hVDRs, including T-box (E98K/E99K), ΔA-box, loop IA, and loop IB mutants. (A) VDRE-binding activity measured by gel mobility shift assay. Lane 1: Free CT5 (osteocalcin VDRE) probe control. Lane 2: Whole cell extract (5 μg protein) from transfected COS-7 cells expressing wild-type hVDR. Lanes 3−6: Extracts from cells expressing the indicated mutant hVDRs. Extracts were incubated with labeled CT5 VDRE probe in the presence of *E. coli*-expressed human RXRα (50 ng). (B) Transcriptional activity of hVDR mutants. COS-7 cells were cotransfected with the VDRE-reporter plasmid $(CT4)_4TKGH$ (3 μg/plate) and the various hVDR expression vectors (5 μg/plate). Transcriptional activity was quantitated by growth hormone radioimmunoassay as described in Methods, and the level of transcription with wild-type hVDR in the presence of 10 nM $1,25(OH)_2D_3$ was arbitrarily set at 100%. In "mock" transfections, no receptor expression plasmid was included. (C) Immunoblot analysis to assess mutant hVDR expression. Lane 1: Mock transfected control. Lanes 2−6 contain extracts (200 μg protein) from cells transfected with the indicated hVDR expression vector. Lane 4: As noted by an asterisk (*), the E98K/E99K receptor cannot be visualized in this Western blot due to a presumed alteration of the 9A7γ antibody epitope.

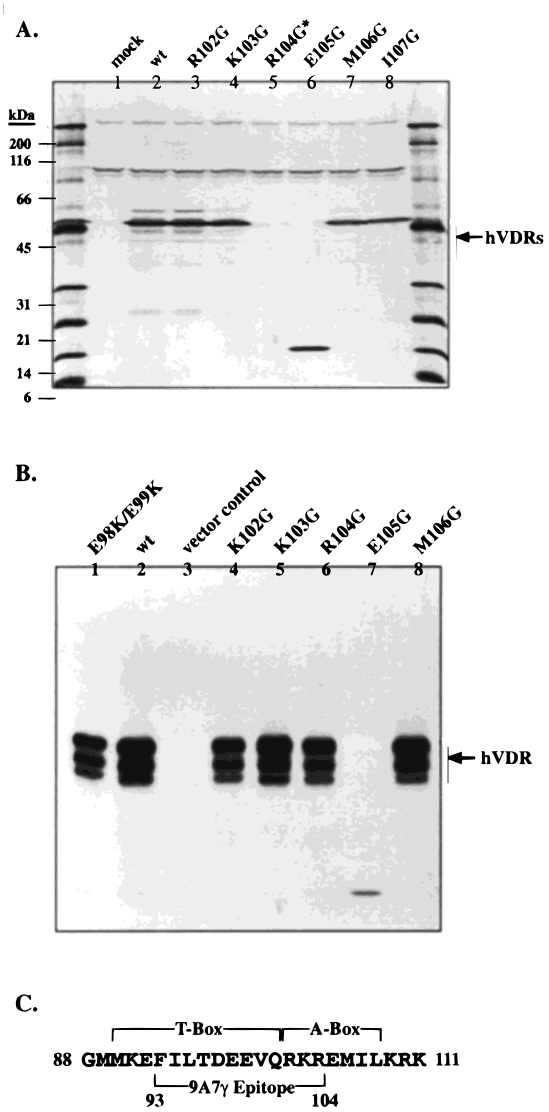

FIGURE 3: Expression and immunoreactivity of mutant hVDRs; redefining the epitope for monoclonal antibody 9A7γ. (A) Expression and immunoreactivity of the indicated mutant hVDRs determined by immunoblot analysis. Equivalent amounts (160 μg protein) of whole cell extracts from transfected COS-7 cells were loaded in each lane. Lane 1 (mock), the expression vector control, contains no hVDR cDNA insert. Arrow at right indicates the migration position of hVDR. Lane 5: Note that R104G, with asterisk (*), is not detected in this Western blot because of 9A7γ antibody epitope inactivation, and E105G is apparently proteolyzed to a 15 kDa immunoreactive hVDR fragment. (B) In vitro transcription/translation of the E98K/E99K and R104G as well as other A-box point mutant hVDRs. Coupled in vitro transcription/translation from the T7 promoter driving hVDR expression in the pSG5hVDR vector (1 μg) was performed using a TNT rabbit reticulocyte lysate kit (Promega, Madison, WI) in the presence of [^{35}S]methionine (see Methods). The arrow indicates the position of hVDR. (C) On the basis of the results in A and B, the epitope for monoclonal antibody 9A7γ (*29*) has been refined to encompass residues 93 to 104.

transcription/translation experiment (Figure 3B) demonstrated that the R104G mutant was synthesized normally, but again the in vitro synthesized E105G mutant VDR was labile to proteolysis (see Discussion).

The data presented so far (Figures 2C, 3A, and 3B), plus the fact that hVDR double mutant K91N/E92Q (Figure 1E) is still reactive to the 9A7γ monoclonal antibody (*27*), allows us to refine slightly the epitope for monoclonal antibody 9A7γ in hVDR, which was originally determined by Pike and associates (*26*, *29*) as encompassing residues 89−105. As depicted in Figure 3C, we now conclude that this epitope traverses from Phe-93 to Arg-104. Apparently, the antibody can tolerate single substitutions within the proposed epitope at Arg-102 and Lys-103 (Figure 3A) as well as the deletion of residues 102−107 (ΔA-box; see Figure 2C). This latter observation is surprising until one considers that, in the ΔA-box deletant, the lost RKR (residues 102−104) triplet is positionally replaced in the primary structure with a KRK (residues 109−111) triplet of similar basic amino acids (Figure 3C). The fact that monoclonal antibody 9A7γ completely blocks hVDR DNA binding in gel mobility shift assays (*27*) is consistent with this epitope involving charged sequences ^{98}EE^{99} and ^{102}RKR^{104}, which were independently shown to be required for DNA binding (Figures 2A and 7B).

Figure 4A shows that point mutant hVDRs at the N-terminal end of the A-box, such as R102G and K103G, are more inhibited in their ability to mediate transactivation by 1,25$(OH)_2D_3$ than are those at the C-terminus of this domain (M106G and I107G). However, as depicted in Figure 4B, each of the A-box point mutants associates almost normally with DNA in a gel mobility shift assay. If the hVDR A-box participates in DNA binding as suggested by Figure 2A, such involvement apparently tolerates the alteration of single key basic residues such as Arg-102 or Lys-103, similar to the flexibility for recognition of VDR by the 9A7γ antibody. Yet the loss of transactivation (Figure 4A) in point mutant hVDRs that associate normally with the VDRE (Figure 4B) suggests that, as in loop I of the first zinc finger, certain residues in the A-box may be directly involved in transactivation. To provide further support for this conclusion, we determined that certain A-box hVDR mutants, especially K103G, function as dominant negative hVDRs (Figure 5). A dominant negative phenotype is consistent with a transcriptionally incompetent VDR that heterodimerizes normally and binds the VDRE/DNA to compete with wild-type VDRs that possess an intact transactivation function.

Next, we evaluated by mutation the role(s) of conserved charged residues N- and C-terminal to the T- and A-box region (see Figure 1E). Alteration of helix B Lys-82 to glutamic acid attenuates hVDR DNA binding and transactivation, whereas these activities of the receptor are unaffected by mutation of Glu-112 (Figure 6, A and B). Altering the three basic residues just C-terminal of the A-box to glycine, specifically in the K109G/R110G/K111G triple mutant, abolishes VDRE binding and transcriptional activation by hVDR (Figure 6, A and B). Similar results were obtained when all three of these basic residues were altered to alanine, which may better preserve the putative α-helical structure in this domain of hVDR (Figure 7, A and B), thus highlighting the fundamental significance of this cluster of three positively charged residues in the functions of VDR. A comparable triple mutation to alanine in the basic cluster at residues 102−104 generates the same hVDR phenotype of absent DNA binding and transactivation (Figure 7, A and B), indicating that these A-box positively charged amino acids constitute a second crucial functional unit in this region of hVDR.

Table 1 lists the properties of all of the hVDR mutants examined in the present experiments, and in a previous study (K91N/E92Q) (*27*). In toto, the results in Table 1 support

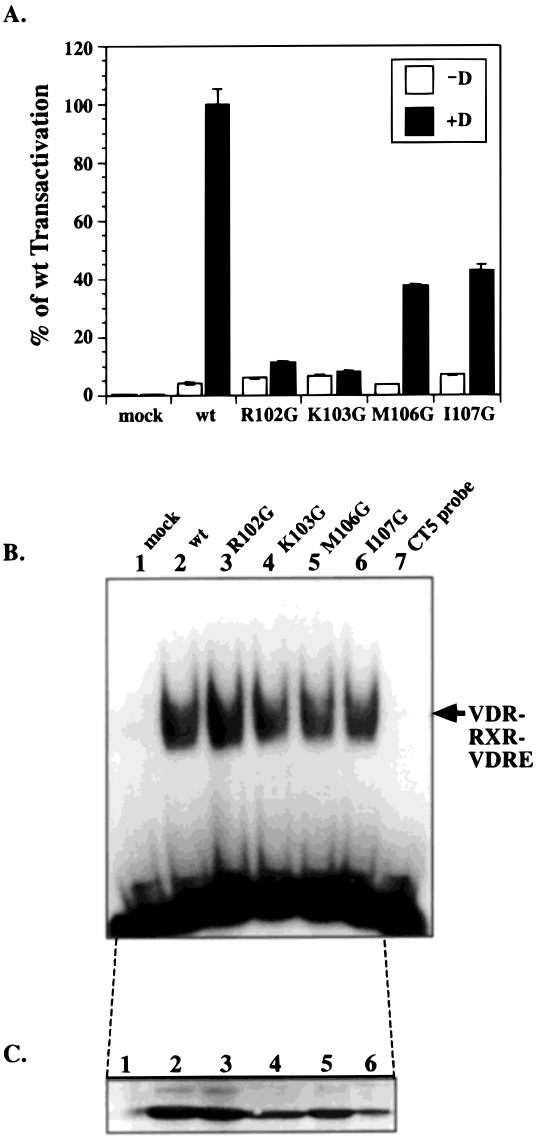

FIGURE 4: Functional characterization of A-box point mutant hVDRs. (A) Transcriptional activity of wild-type, and A-box point mutant hVDRs using a VDRE reporter. COS-7 cells were cotransfected with a VDRE-reporter plasmid $(CT4)_4TKGH$ (2 μg/plate), carrier pTZ18U DNA (23 μg/plate), and the various hVDR expression vectors (5 μg/plate). Transcriptional activation was quantitated using a growth hormone radioimmunoassay, with the level of transcription by wild-type hVDR in the presence of 10 nM $1,25(OH)_2D_3$ arbitrarily set at 100%. In mock transfections, no receptor expression plasmid was included. (B) DNA-binding activity was measured by a gel mobility shift assay. Lane 1−6: Cell extracts (10 μg) from untransfected (lane 1) or transfected (lanes 2−6) COS-7 cells were incubated with purified, *E. coli*-expressed RXRα (50 ng) and CT5 (osteocalcin VDRE) probe. Lane 7 contains labeled probe only. (C) Immunoblot analysis to assess hVDR expression. Whole cell extracts (80 μg) corresponding to lanes 1−6 of panel B were evaluated by Western blotting as described in the legend to Figure 1D.

an assignment of the 9A7γ epitope as spanning amino acids 93−104 (Figure 3C), with residues 102 and 103 not essential for the integrity of the epitope. To confirm this conclusion and ensure that those hVDR mutants not visualized with 9A7γ (Table 1) were actually expressed in COS-7 cells, immunoblotting was performed using a polyclonal antiserum directed against the C-terminus of hVDR. The R104A, R104G, and R102A/K103A/R104A mutant hVDRs were all

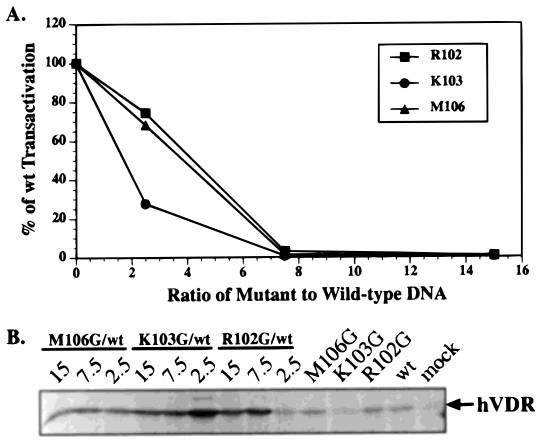

FIGURE 5: Dominant negative activity of R102G, K103G, and M106G A-box mutant hVDRs. (A) COS-7 cells were cotransfected with the reporter plasmid $(CT4)_4TKGH$ (2 μg/plate) and the amount of transfected mutant hVDR expression vectors was increased (2.5 μg/plate, 7.5 μg/plate, and 15 μg/plate) relative to the wild-type hVDR expression vector (1 μg/plate). Sixteen hours after transfection, cells were incubated in the presence of 10 nM $1,25(OH)_2D_3$ hormone for an additional 24 h prior to harvesting and growth hormone assay. (B) Immunoblot analysis to assess hVDR expression (indicated by the arrow) in this representative experiment. R102G/wt, M106G/wt, and K103G/wt, refer to the ratios of each mutant to wild-type receptor expression plasmids used in each transfection.

expressed equivalently to wild-type receptor, and only E98K/E99K was reduced somewhat in expression to approximately 50% of wild-type levels (data not shown). However, this partial reduction in E98K/E99K hVDR expression cannot account for its near total absence of DNA binding, transactivation, and detectability by the 9A7γ monoclonal antibody (Figure 2). In addition to Glu-98/Glu-99, other residues required for competent heterodimerization/VDRE binding are Lys-91/Glu-92, and at least one basic residue in each of the 102−104 and 109−111 positively charged clusters. Finally, none of the tested mutants in the C-terminal extension of the zinc finger region mediated optimal transactivation except E112G (Table 1), with individual residues in the two basic clusters appearing to be more significant to transcription than DNA binding per se.

DISCUSSION

The present experiments (summarized in Table 1) clearly indicate a role for the C-terminal extension of the zinc finger region in the association of hVDR with the classic VDRE from the rat osteocalcin gene and define the C-terminal boundary of the DNA-binding function of VDR as extending to Lys-111. The VDR CTE characterized herein overlaps the previously described T- and A-box regions in mRXRβ and the orphan receptor NGFI−B, respectively (*20*), but contains a cluster of three essential basic residues (109−111) located C-terminal of the A-box, as well as a distinctive pattern of functional charged amino acids within the T- and A-boxes. The current results expand previous studies that also suggested the importance of the hVDR CTE, specifically Lys-91 and Glu-92 in the T-box region, in receptor heterodimerization, and responsive element recognition (*11*, *27*). Together, these findings distinguish VDR from the type I homodimerizing receptors, such as GR and ER, wherein the

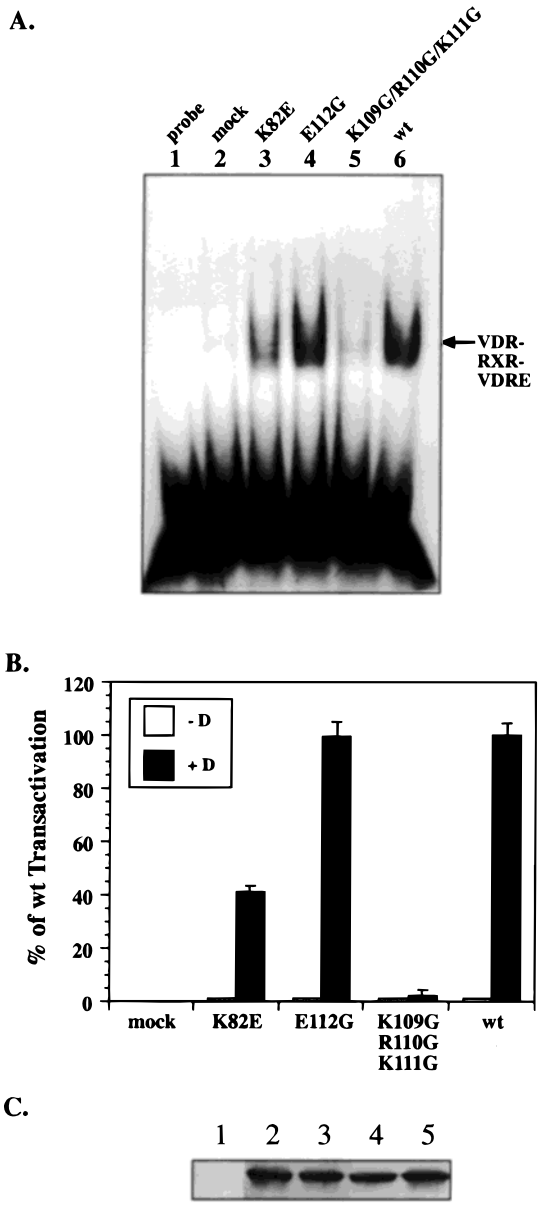

FIGURE 6: Functional evaluation of A-box flanking residues. (A) DNA-binding activity as assessed by gel mobility shift assay. Lane 2: Whole cell extracts (10 μg protein) from mock transfected COS-7 cells. Lanes 3−6: Cells cotransfected with the indicated mutant hVDR were incubated with the ^{32}P-labeled CT5-VDRE probe for 30 min at room temperature in the presence of purified, *E. coli*-expressed RXRα (50 ng). (B) Transcriptional activity of hVDR mutated at Lys-82 as well as at residues immediately C-terminal of the A-box. COS-7 cells were cotransfected with either wild-type or mutant pSG5hVDR expression plasmids (2 μg/plate), along with the $(CT4)_4$TKGH reporter (6 μg/plate). The amount of growth hormone secreted into the media was compared with the amount in cultures receiving wild-type hVDR and 10^{-8} M $1,25(OH)_2D_3$, which was arbitrarily set at 100%. (C) Expression of wild-type and mutant hVDRs determined by Western blot of lysates from cells transfected as in B. Lane 1: Mock transfection. Lane 2: K82E. Lane 3: E112G. Lane 4: K109G/R110G/K111G. Lane 5: Wild-type hVDR.

P-box, D-box, and other segments solely within the zinc finger motif confer the DNA-binding activity and specificity (*30*, *31*). Further, certain single point mutations in the hVDR CTE, while allowing for apparently normal DNA binding, severely affected transactivation by the liganded receptor. Thus, this CTE domain of hVDR also appears to contribute

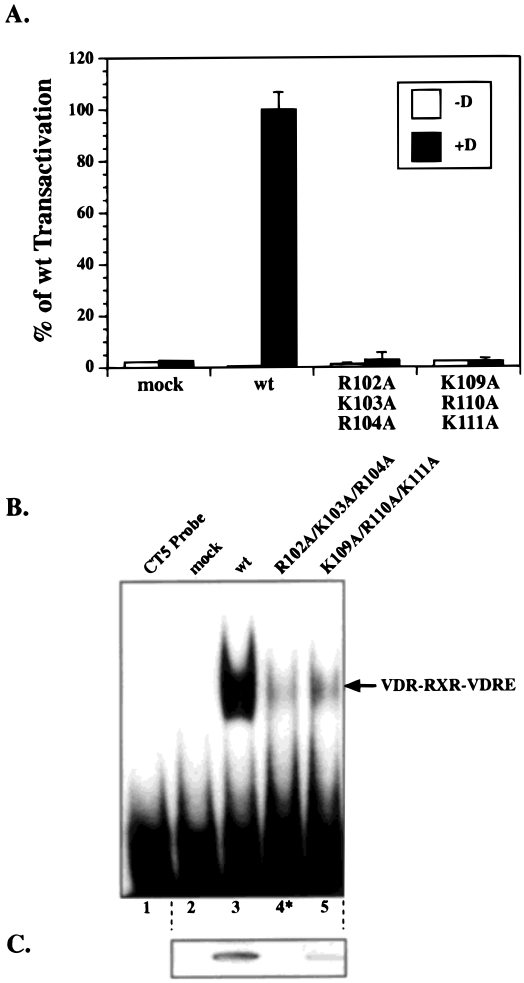

FIGURE 7: Properties of R102A/K103A/R104A and K109A/R110A/K111A mutant hVDRs. (A) Transcriptional activity measured by hGH assay. COS-7 cells were cotransfected with either wild-type or mutant pSG5hVDR expression plasmids (2 μg/plate), along with the $(CT4)_4$TKGH reporter construct (6 μg/plate). The amounts of growth hormone secreted into the media were compared with the amounts in cultures receiving wild-type hVDR and 10^{-8} M $1,25-(OH)_2D_3$, which was arbitrarily set at 100%. (B) DNA-binding activity via the gel mobility shift assay. Whole cell extracts (10 μg protein) from untransfected COS-7 cells (lane 2) or cells transfected with wild-type (lane 3), R102A/K103A/R104A (lane 4), or K109A/R110A/K111A hVDR (lane 5) were incubated with 0.5 ng of the ^{32}P-labeled CT5 VDRE probe for 30 min at room temperature in the presence of purified, *E. coli*-expressed RXRα (50 ng). (C) Expression of wild-type and mutant hVDRs as determined by Western blot of lysates from cells transfected in B. Lane 4: As indicated by an asterisk (*), the R102A/K103A/R104A protein cannot be detected in this immunoblot because the 9A7γ epitope covers residues 93−104, but its expression has been verified by visualization with a separate polyclonal anti-VDR antibody (data not shown).

transcriptional activation functions independent of DNA binding.

The A-box region of the CTE was originally described for the orphan receptor NGFI-B (also called *nur77*) (*20*), which binds as a monomer to a response element consisting of a single hexanucleotide half-site plus a 5′ extension of at least two base pairs (e.g., *AA*AGGTCA). Removal of the A-box region of NGFI-B severely affected DNA binding to the AAAGGTCA element (*20*). Further, attachment of the T- and A-boxes from RXR to a truncated NGFI-B resulted in a chimeric receptor capable of binding as a dimer to a DR+1 RXR responsive element (RXRE) (*20*). Conversely,

replacement of the A-box in RXR by the corresponding region in NGFI-B allowed the chimeric receptor to bind to the NGFI-B element as a monomer. Thus, the CTE of NGFI-B appears to mediate recognition of the 5′ AA extension in the NGFI-B responsive element, even when the entire zinc finger motif of NGFI-B is replaced by that of RXR. In analogous experiments (*27*), we previously showed that altering either the P- or D-box in VDR to that of GR did not significantly impair VDR heterodimeric DNA-binding or transactivation ability. These studies highlight the significance of the CTE also in the type II nuclear receptors that heterodimerize with RXR.

A PCR-based random selection method was used by Wilson et al. (*20*) to further investigate which A-box residues were responsible for interaction with the 5′ extension of the hexanucleotide element, and it was found that the presence of at least three positively charged residues in the first five positions of the A-box was required for proper DNA contact (*20*). Comparison of the A-box sequence of NGFI-B with the corresponding regions of other nuclear receptors that bind as monomers (e.g., human estrogen-receptor related receptor 2 (hERR2), hRORα, or hRev-Erb) shows that all of these receptors contain three basic residues in or immediately adjacent to the A-box, although the exact placement of these residues can vary ± one position between receptors (Figure 8). Taken together, these results imply a crucial role for the A-box, especially its basic residues, in the recognition of bases 5′ of the consensus hexanucleotide half-element. The fact that VDR possesses three basic residues (102−104) at the N-terminus of its A-box (Figure 8), which are required for DNA binding (Figure 7B), indicates that this portion of the A-box in VDR may subserve a similar role.

There is independent evidence that the A-box may function in heterodimer-forming nuclear receptors in addition to VDR. In the crystal structure determined by Rastinejad et al. (*11*) for the hRXRα-hTR*β* complex bound to a DR+4 sequence, there exists an extensive α-helix in TR beginning midway through the T-box and extending 12 residues C-terminal of the A-box (Figure 8). Further, nine DNA−protein contacts occur in this α-helix, six of which involve basic residues that are positionally conserved in all TRs described to date (see Figure 8 for selected examples). These results unambiguously define a role in DNA binding for positively charged residues within, and even beyond, the A-box, in a nuclear receptor closely related to VDR.

Rastinejad et al. (*11*) further proposed a role for the CTE in responsive element spacer discrimination by demonstrating, using computer generated models, that the long α-helix in the CTE of TR would cause steric hindrance to RXR binding on a half-site less than 4 bp upstream of the TR half-element. Further evidence for this interpretation includes two earlier investigations (*18*, *32*) in which it was concluded that the CTEs of TR and RAR are at least partially responsible for the spacing discrimination displayed by these receptors on their cognate DR+4 and DR+5 elements, respectively.

A direct application of the above interpretations to VDR is complicated, not only by incomplete conservation of the relevant basic residues between VDR, TR, and RAR, but also by the fact that each of these receptors binds to responsive elements with different spacers. Nevertheless, an attempt was made by Rastinejad et al. (*11*) to model VDR−RXR on its DR+3 element using the TR−RXR−DR+4 X-ray crystallographic coordinates. While these authors focused on dimer contacts between VDR and RXR in their analysis (hypothesizing a role for VDR Lys-91 and Glu-92 as RXR contacts), a putative α-helix containing CTE residues C-terminal of Glu-92 in hVDR is evident in their RXR−VDR−DR+3 model. This α-helix seems to interact with DNA, apparently in the spacer region (see ref *11*, p 209, Figure 4b). The difference between the RXR−TR−DR+4-bound receptor heterodimer, and RXR−VDR modeled on a DR+3 as reported by these authors, appears to be in a "shifting" of receptor dimer contacts, and also a "readjustment" in the location of receptor α-helices relative to other structural components in order to accommodate differences in the spacing between half-sites of the responsive elements (*11*).

As illustrated in Figure 8, the conserved regions within the CTEs of nuclear receptors do indeed seem to shift in a regular pattern that appears to be related to the spacer length of the cognate responsive element. Thus, those receptors that bind to the 3′ half-site of DR+1 elements, namely, RXR (as part of a homodimer) and HNF4, display sequence conservation extending C-terminal from the zinc fingers only to near the end of the T-box. RARs, which bind as RXR heterodimers to DR+2 elements, possess a stretch of four conserved lysines that lie progressively more C-terminal and straddle the T/A-box junction. In contrast, receptors that bind to the 3′ half-site of DR+3 elements, i.e., VDR (*33*) and PXR (*34*), display conservation to three positions C-terminal of the A-box. The most striking feature of the CTE in the DR+3 receptors, including VDR, is the occurrence of two more C-terminal, conserved clusters of basic amino acids (Figure 8), each of which contains at least one positively charged residue absolutely essential for VDRE binding by VDR (Table 1). Finally, TRs, which bind to DR+4 elements, show strong amino acid conservation extending 13 positions C-terminal to the A-box and display an apparent "C-terminal shift" relative to VDR in similar conserved clusters of basic amino acids (Figure 8).

One might expect from this trend that RARs, which not only bind to DR+2 DNA elements, but also to DR+5 elements, might possess CTEs that are more extensive than those of TRs, and that contain basic clusters shifted even more C-terminal. However, as can be seen from Figure 8, this is not the case. In a model of RAR−RXR on a DR+5 (*11*), no interactions are shown between CTE residues of RAR and DNA. This is consistent with the fact that, in a sequence comparison, the CTEs found in RARs resemble those in the monomer and DR+1 binding receptors more than those in TRs (Figure 8). Thus, it is possible to conclude that while RAR is capable of binding to both DR+5 and DR+2 elements, the RAR CTE is designed primarily to interact with, and determine, the DR+2 spacer motif. With a DR+5 motif, steric hindrance is likely relaxed as it may be in homodimeric nuclear receptors associating with an inverted repeat separated by three base pairs, thereby obviating the need for CTE−DNA interactions.

Whether the DR+3 (e.g., VDR and PXR/ONR) receptors possess α-helices in their CTE regions is not established because of an absence of structural data, although proline residues do not occur in xONR, PXRs, and VDRs until 29−34 positions C-terminal of helix B (Figure 8). Further indirect evidence of an α-helix in the A-box region of VDR is our

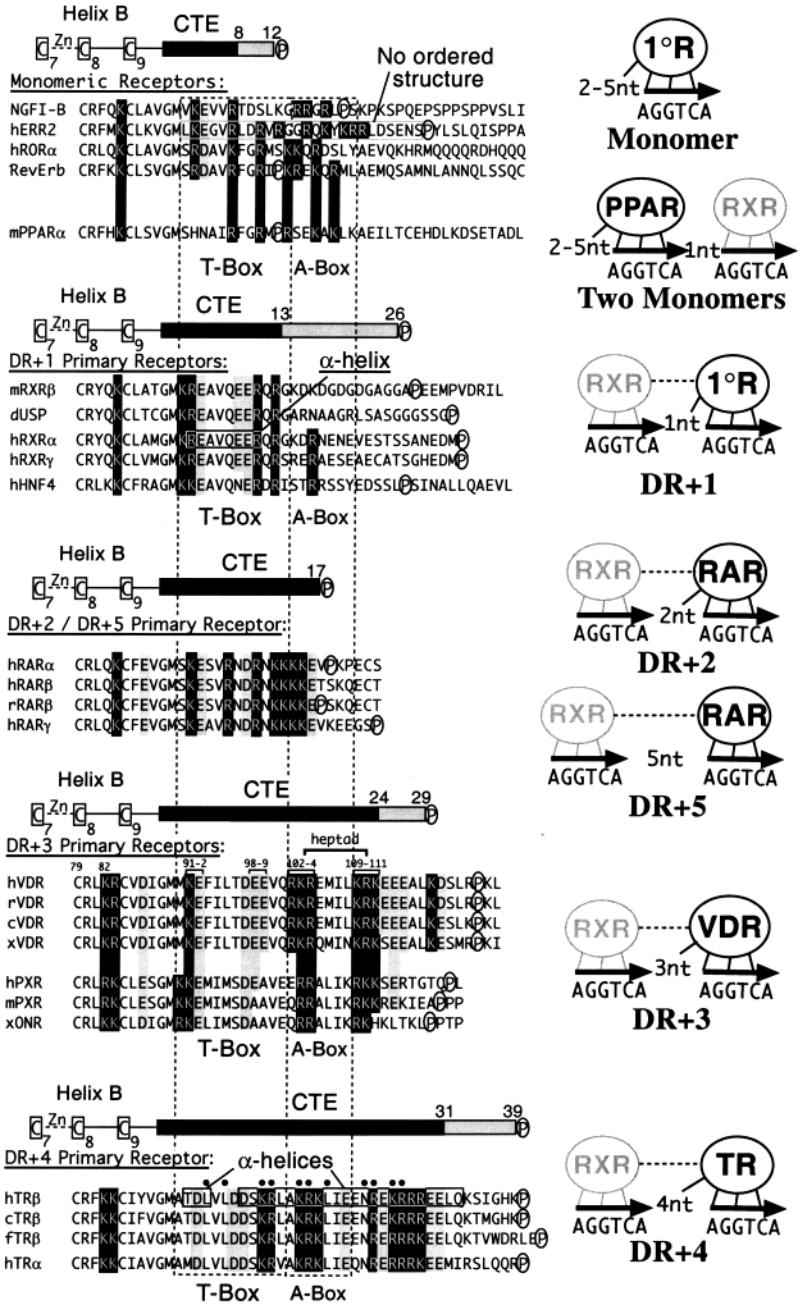

FIGURE 8: CTEs of selected nuclear hormone receptors, arranged by DNA-binding-site preference. Cartoons at right depict the primary receptor (1°R), such as RAR, VDR, or TR, binding to the "generic" hexanucleotide half-site (AGGTCA) and also interacting in most cases with flanking nucleotides. The RXR coreceptor is shown in gray. DR+1, DR+2, etc., refer to direct repeat elements with various spacers. At left are selected CTE sequences of receptors that bind to each response element. Sequences begin with helix B in the crystal structure of the DNA-binding domains of hTRβ and hRXRα, which encompasses the seventh, eighth, and ninth conserved cysteines of the zinc finger motif. The CTE region of each receptor, as defined herein, begins immediately C-terminal to helix B at a universally conserved "GM" amino acid pair. That portion of the CTE which is well conserved within a given group of receptors is denoted by a horizontal black bar above the sequences, with the position number C-terminal to helix B given above the right end of the bar. Also denoted by its numbered position, C-terminal to helix B is the balance of each CTE depicted as a gray bar extending from the black bar. The position of the first proline residue within a group (circled in the sequence) defines the end of the CTE according to the present model. Conserved basic residues are shown in white letters over a solid black fill. Conserved acidic residues are in black letters over gray shading. Other features are as follows: (a) that portion of the CTE of the hERR2 orphan receptor shown to be without ordered structure (*21*) is boxed with a gray line; (b) residues corresponding to the proposed A- and T-boxes (*20*), originally defined for NGFI-B orphan receptor and mRXRβ, respectively, are boxed for all receptors with dashed lines; (c) the hVDR sequence is annotated with position numbers from the published sequence (*41*); (d) α-helices within the CTE, as determined for hRXRα (*19*, *42*), and for hTRβ (*11*), are boxed inside solid black lines; (e) DNA contacts in the CTE of the hTRβ−RXR−TRE crystal structure (*11*) are indicated by black dots. Genbank accession numbers for sequences are as follows (lower case "h" at the beginning indicates a human sequence): hNGFI-B (AAB33999), hERR2 (CAA35779), hRORα (U04897), hRevErb (P20393), mouse PPARα (P23204), mouse RXRβ (BAA04858), *Drosophila* USP (X53417), hRXRα (X52773), hRXRγ (P48443), hHNF4 orphan receptor (CAA54248), hRARα (A29491), hRARβ (NP_000956), rat RARβ (CAA05769), and hRARγ (AAA52692), hVDR (NP_000367), rat VDR (S24174), chicken VDR (AAB62579), *Xenopus* VDR (AAB58585), hPXR (AF061056), mouse PXR (AAC39964), xONR (the *Xenopus* homologue of PXR) (CAA53006), hTRβ (TVHUAR), chicken TRβ (TVCHTB), Japanese flounder TRβ (BAA08201), hTRα (CAA38749).

observation (Figure 3, A and B) that replacement of Glu-105 with glycine, potentially disrupting a putative α-helical region, caused hVDR to be proteolyzed to a 15 kDa immunoreactive fragment. Ray and colleagues (*35*) have reported that Glu-105 lies within a critical VDR domain for the binding and presumed stabilization of the secondary structure of apoVDR by bacterial DnaK as well as by possible mammalian heat shock protein homologues. Therefore, it is probable that Glu-105 is essential to the secondary structure of VDR, both because it is retained as an α-helix-compatible glutamine or alanine in lower VDRs (i.e., *Xenopus*) and in other DR+3 receptors, such as PXR, and because its alteration to glycine likely generates a dominant negative VDR that would be deleterious to the cell as is the case for mutations to glycine in residues 103 and 106 (Figure 5A). Further, given the 3.6 residue periodicity of an α-helix, it can be seen from Figure 8 that many of the conserved basic residues in VDR, PXR, and RAR would appear on the same face of the helix (assuming such a structure is present), creating a suitable interface for interactions with the phosphate backbone of DNA. This concept certainly applies to the two basic clusters in VDR (residues 102−104 and 109−111), which exhibit perfect heptad spacing (Figure 8). Finally, comparisons of RXR, RAR, VDR, and TR are consistent with, and indeed suggestive of, the existence of α-helical elements that feature basic residues on one side to interact with DNA, and whose length varies according to the spacer of the direct repeat responsive element.

We, therefore, propose a working model for the molecular role of the VDR A-box and its C-terminal extension of three basic residues, based not only on inferences from hTRβ crystallographic data, but also from patterns of conserved charged residues whose functions have been explored herein by site-directed mutagenesis. Given the above examples of NGFI-B and TR, we infer that the CTE of VDR may interact with bases in the 3-bp spacer of its responsive element. Previous results of MacDonald et al. (*36*), who reported interaction between baculovirus-expressed hVDR and a G nucleotide in position #3 of the spacer in the rat osteocalcin VDRE, and evidence from random nucleotide selection experiments that yielded a G in this position of the VDRE spacer (*37*, *38*) are consistent with this interpretation. Although a role for the VDR CTE in half-site determination cannot be concluded directly from the present data, it is striking that the unique pattern of basic amino acid clusters in VDR is positionally conserved only in nuclear receptors that bind DR+3 DNA elements (i.e., PXR and ONR), but not in receptors that bind to other motifs (Figure 8). Thus, the array of basic clusters in the VDR CTE, which have been shown herein to possess functional significance, likely form contacts with the DR+3 spacer and may also discriminate against spacers of other lengths.

Recent studies of peroxisome proliferator-activated receptors (PPARs) provide independent support for the above model. PPARs are unique in that they bind noncooperatively to DR+1 elements, with a polarity opposite to that of most type II nuclear receptors, i.e., with the RXR coreceptor residing on the 3′ half-element. PPARs require a 2−5 bp 5′ extension of the 5′ half-element, and it is the CTE of PPARs that contributes significantly to both the specificity and polarity of this DNA binding (*39*). Therefore, PPARs utilize their CTE, which is strikingly similar in sequence to that of hRev-Erb and other monomer binding receptors (Figure 8), to contact a 5′ extension of the cognate half-element, behaving essentially like monomeric receptors (see Figure 8). We propose that VDR functions analogously with respect to its CTE, but that the 5′ extension is actually the spacer separating the 3′ VDR half-site from the 5′ RXR half-site, with the fundamental difference between VDR and PPAR being that, because of different polarity, VDR binds to its responsive element cooperatively as an RXR heterodimer.

The present results (Figure 2), involving the alteration of Glu-98 and Glu-99 within the hVDR T-box, suggest that essential functions of the CTE are not limited to basic residues, but may be performed by acidic residues as well. The hVDR E98K/E99K double mutant is severely compromised in both DNA binding (Figure 2A) and transactivation (Figure 2B), even though it can be expressed at reasonable levels, both in vitro (Figure 3B) and in COS-7 cells (data not shown). A role of acidic residues in directly contacting DNA has precedent, with perhaps the most prominent example being the Glu residue in the conserved *E*GxxG motif of the P-box in the first zinc finger of ER and TR (*11*, *30*). However, except for the Glu-92 RXR contact residue in VDR (and the corresponding Asp in TR), the role of acidic residues in the CTE has not previously been reported.

The working model of the VDR CTE presented above can be used as a basis for further experimentation, such as an investigation of potential exposed interfaces of VDR that serve as protein−protein contacts for the docking of other transcription factors or coactivators (or even corepressors). In fact, Lys-103 mutations in VDR bind DNA efficiently, in vitro, but are incapable of effective transactivation (Table 1). One explanation, suggested by the position of this residue within the 9A7γ monoclonal antibody epitope, is that this residue may be a component of an exposed surface, potentially part of a protein−protein interface with a coactivator that facilitates transcription. We hypothesize that Lys-103 mutants may still be able to bind DNA via the Arg-102 and Arg-104 residues, yet could be distorted such as to preclude the proper conformation for transactivation. An alternative explanation is that Lys-103 may be part of a second bipartite nuclear localization signal for VDR (*13*), as has been proposed by Luo et al. (*40*). Ultimately, however, a complete appreciation of the structural elements in the CTE of VDR must await X-ray crystallography or NMR data of this region of VDR, preferably as a heterodimer with the DNA binding domain of RXR on a DR+3 element.

ACKNOWLEDGMENT

We thank Milan Uskokovic of Hoffmann-LaRoche Inc. for kindly providing 1,25-dihydroxyvitamin D_3 for our studies. The authors express appreciation to Sanford H. Selznick for his technical expertise and patience in the preparation of figures for this manuscript. We also wish to thank Michelle Thatcher and Lenore Remus for excellent technical assistance.

REFERENCES

1. Mangelsdorf, D. J., and Evans, R. M. (1995) *Cell 83*, 841−850.
2. Haussler, M. R., Whitfield, G. K., Haussler, C. A., Hsieh, J.-C., Thompson, P. D., Selznick, S. H., Encinas Dominguez, C., and Jurutka, P. W. (1998) *J. Bone Miner. Res. 13*, 325−349.

3. DeMay, M. B., Gerardi, J. M., DeLuca, H. F., and Kronenberg, H. M. (1990) *Proc. Natl. Acad. Sci. U.S.A. 87*, 369−373.
4. Ozono, K., Liao, J., Kerner, S. A., Scott, R. A., and Pike, J. W. (1990) *J. Biol. Chem. 265*, 21881−21888.
5. Terpening, C. M., Haussler, C. A., Jurutka, P. W., Galligan, M. A., Komm, B. S., and Haussler, M. R. (1991) *Mol. Endocrinol. 5*, 373−385.
6. Noda, M., Vogel, R. L., Craig, A. M., Prahl, J., DeLuca, H. F., and Denhardt, D. T. (1990) *Proc. Natl. Acad. Sci. U.S.A. 87*, 9995−9999.
7. Cao, X., Ross, F. P., Zhang, L., MacDonald, P. N., Chappel, J., and Teitelbaum, S. L. (1993) *J. Biol. Chem. 268*, 27371−27380.
8. Hahn, C. N., Kerry, D. M., Omdahl, J. L., and May, B. K. (1994) *Nucleic Acids Res. 22*, 2410−2416.
9. Zierold, C., Darwish, H. M., and DeLuca, H. F. (1994) *Proc. Natl. Acad. Sci. U.S.A. 91*, 900−902.
10. Haussler, M. R., Jurutka, P. W., Hsieh, J.-C., Thompson, P. D., Haussler, C. A., Selznick, S. H., Remus, L. S., and Whitfield, G. K. (1997) in *Vitamin D* (Feldman, D., Glorieux, F., and Pike, J. W., Eds.) pp 149−177, Academic Press, San Diego.
11. Rastinejad, F., Perlmann, T., Evans, R. M., and Sigler, P. B. (1995) *Nature 375*, 203−211.
12. Rut, A. R., Hewison, M., Kristjansson, K., Luisi, B., Hughes, M. R., and O'Riordan, J. L. H. (1994) *Clin. Endocrinol. (Oxf) 41*, 581−590.
13. Hsieh, J.-C., Shimizu, Y., Minoshima, S., Shimizu, N., Haussler, C. A., Jurutka, P. W., and Haussler, M. R. (1998) *J. Cell. Biochem. 70*, 94−109.
14. Hsieh, J.-C., Jurutka, P. W., Galligan, M. A., Terpening, C. M., Haussler, C. A., Samuels, D. S., Shimizu, Y., Shimizu, N., and Haussler, M. R. (1991) *Proc. Natl. Acad. Sci. U.S.A. 88*, 9315−9319.
15. Hsieh, J.-C., Jurutka, P. W., Nakajima, S., Galligan, M. A., Haussler, C. A., Shimizu, Y., Shimizu, N., Whitfield, G. K., and Haussler, M. R. (1993) *J. Biol. Chem. 268*, 15118−15126.
16. Lundback, T., Zilliacus, J., Gustafsson, J. A., Carlstedt-Duke, J., and Hard, T. (1994) *Biochemistry 33*, 5955−5965.
17. Mader, S., Chambon, P., and White, J. H. (1993) *Nucleic Acids Res. 21*, 1125−1132.
18. Zechel, C., Shen, X.-Q., Chambon, P., and Gronemeyer, H. (1994) *EMBO J. 13*, 1414−1424.
19. Lee, M. S., Kliewer, S. A., Provencal, J., Wright, P. E., and Evans, R. M. (1993) *Science 260*, 1117−1121.
20. Wilson, T. E., Paulsen, R. E., Padgett, K. A., and Milbrandt, J. (1992) *Science 256*, 107−110.
21. Sem, D. S., Casimiro, D. R., Kliewer, S. A., Provencal, J., Evans, R. M., and Wright, P. E. (1997) *J. Biol. Chem. 272*, 18038−18043.
22. Giguere, V., McBroom, L. D., and Flock, G. (1995) *Mol. Cell. Biol. 15*, 2517−2526.
23. Harding, H. P., and Lazar, M. A. (1993) *Mol. Cell. Biol. 13*, 3113−3121.
24. Hsieh, J.-C., Nakajima, S., Galligan, M. A., Jurutka, P. W., Haussler, C. A., Whitfield, G. K., and Haussler, M. R. (1995) *J. Steroid Biochem. Mol. Biol. 53*, 583−594.
25. Freedman, L. P., and Towers, T. L. (1991) *Mol. Endocrinol. 5*, 1815−1826.
26. McDonnell, D. P., Scott, R. A., Kerner, S. A., O'Malley, B. W., and Pike, J. W. (1989) *Mol. Endocrinol. 3*, 635−644.
27. Hsieh, J.-C., Jurutka, P. W., Selznick, S. H., Reeder, M. C., Haussler, C. A., Whitfield, G. K., and Haussler, M. R. (1995) *Biochem. Biophys. Res. Commun. 215*, 1−7.
28. Bradford, M. M. (1976) *Anal. Biochem. 72*, 248−254.
29. Pike, J. W., Kesterson, R. A., Scott, R. A., Kerner, S. A., McDonnell, D. P., and O'Malley, B. W. (1988) in *Vitamin D: Molecular, Cellular and Clinical Endocrinology* (Norman, A. W., Schaefer, K., Grigoleit, H.-G., and von Herrath, D., Eds.) pp 215−224, Walter de Gruyter & Co., Berlin, New York.
30. Umesono, K., and Evans, R. M. (1989) *Cell 57*, 1139−1146.
31. Schwabe, J. W. R., Chapman, L., Finch, J. T., and Rhodes, D. (1993) *Cell 75*, 567−578.
32. Kurokawa, R., Yu, V. C., Näär, A., Kyakumoto, S., Han, Z., Silverman, S., Rosenfeld, M. G., and Glass, C. K. (1993) *Genes Dev. 7*, 1423−1435.
33. Jin, C. H., and Pike, J. W. (1996) *Mol. Endocrinol. 10*, 196−205.
34. Lehmann, J. M., McKee, D. D., Watson, M. A., Willson, T. M., Moore, J. T., and Kliewer, S. A. (1998) *J. Clin. Invest. 102*, 1016−23.
35. Swamy, N., Mohr, S. C., Xu, W., and Ray, R. (1999) *Arch. Biochem. Biophys. 363*, 219−226.
36. MacDonald, P. N., Haussler, C. A., Terpening, C. M., Galligan, M. A., Reeder, M. C., Whitfield, G. K., and Haussler, M. R. (1991) *J. Biol. Chem. 266*, 18808−18813.
37. Colnot, S., Lambert, M., Blin, C., Thomasset, M., and Perret, C. (1995) *Mol. Cell. Endocrinol. 113*, 89−98.
38. Nishikawa, J., Kitaura, M., Matsumoto, M., Imagawa, M., and Nishihara, T. (1994) *Nucleic Acids Res. 22*, 2902−2907.
39. Hsu, M. H., Palmer, C. N., Song, W., Griffin, K. J., and Johnson, E. F. (1998) *J. Biol. Chem. 273*, 27988−27997.
40. Luo, Z., Rouvinen, J., and Mäenpää, P. H. (1994) *Eur. J. Biochem. 223*, 381−387.
41. Baker, A. R., McDonnell, D. P., Hughes, M. R., Crisp, T. M., Mangelsdorf, D. J., Haussler, M. R., Pike, J. W., Shine, J., and O'Malley, B. W. (1988) *Proc. Natl. Acad. Sci. U.S.A. 85*, 3294−3298.
42. Holmbeck, S. M., Foster, M. P., Casimiro, D. R., Sem, D. S., Dyson, H. J., and Wright, P. E. (1998) *J. Mol. Biol. 281*, 271−284.

BI9916574